Four-dimensional imaging in radiotherapy for lung cancer patients

Wolthaus, J.W.H.

Publication date
2009

Document Version
Final published version

7

Dose accumulation and evaluation

Effects of respiration-induced anatomy variations on dose distributions

V. Mexner
J.W.H. Wolthaus
M. van Herk
E.M.F. Damen
J.J. Sonke

International Journal of Radiation Oncology, Biology and Physics 2009
Accepted for publication

Abstract

Purpose To investigate the effect of respiration-induced anatomy (geometry and density) variations on the estimated dose to moving structures, and consequently evaluating the necessity of using a full four-dimensional (4D) treatment-planning optimization.

Methods and Materials For ten patients, with large tumor motion (median = 1.9 cm, range 1.1-3.6 cm), the clinical treatment plan designed on the mid-ventilation (MidV) CT was recalculated on all 4D CT frames. The cumulative dose was determined by transforming the doses of all breathing phases using deformable registration to the MidV geometry, and then averaging the result. To study the effect of density variations, this cumulative dose was compared to the accumulated result after similarly deforming the planned (3D) MidV dose in each respiratory phase by the same transformation (i.e., “blurring the dose”). Geometry variations were evaluated by comparison to the static MidV dose distribution.

Results The accumulated tumor doses including and excluding density variations were almost identical. Relative differences in minimum GTV dose were below 2% for all patients. For the lung, the differences were even smaller; relative differences in mean lung dose and V20 were below 0.5% and 1%, respectively.

Conclusions The effect of respiration-induced density variations on the delivered dose is very small. Therefore, planning on the MidV CT with dose-blurring according to tumor motion, is an appropriate estimate of the full accumulated 4D dose. Moreover, when using a proper margin to account for geometrical uncertainties such as setup, baseline and respiration uncertainties, the effect of geometry variation to the delivered dose is also small.

1. Introduction

Substantial respiration-induced anatomy changes have been observed in the thoracic region. Breathing causes motion, deformation and density changes in the tumor and the organs-at-risk (OAR; e.g., lungs) as well as other structures (e.g., rib cage). Therefore, a four-dimensional (4D) approach, accounting for moving structures in time, is pursued by many studies for radiotherapy of lung cancer (eg. [1]). Consequently, 4D scanning, planning and treatment delivery are being investigated by several institutions [2-4].

A four-dimensional computed tomography (4D CT) scan is used to represent the changing patient anatomy over the respiratory cycle [5]. By employing an external breathing sensor the CT data (oversampled 4D data) are sorted into multiple three-dimensional (3D) CTs of the different breathing phases. The geometrical relationship between phases can be evaluated by local rigid or deformable registration [6-8].

There exist various methods which incorporate, to different extent, 4D CT information into treatment-planning for better dose prediction of moving structures [1,9]. Full 4D treatment-planning that utilizes the CTs of all breathing phases for dose optimization, is currently not included in most treatment-planning systems. Alternative more simple methods perform a 3D planning on a representative scan, e.g a mean density CT (in combination with a maximum intensity projection –MIP– CT) [9] or mid-ventilation (MidV) CT. Tumor motion is then accounted for with an internal target volume (ITV) or planning target volume (PTV).

To better understand the differences between the 3D and 4D approaches, it is important to realize that respiratory motion has two effects on the dose to moving structures. First, respiration induces structures to move in space, receiving dose at different positions and possibly with a changing shape. This represents *respiration-induced geometry variations*. Second, the dose itself is influenced by moving structures since the density changes over the breathing cycle affect the radiation delivery. This is associated with *respiration-induced density changes*.

In a full 4D dose accumulation approach (accumulated over the 4D trajectory) the two effects are taken into account, that is the tumor and lung trajectory (i.e., geometry variations) as well as the dose changes due to density variations for all phases. A 3D treatment-planning approach, on the other hand, ignores the density changes while the geometry variations are included via the ITV and/or PTV margin. As the geometry variations are then only indirectly taken into account, the effect of density variations can not be quantified by a straightforward comparison. Note that, to check if the planned dose (3D/4D) is an adequate estimate of the actually delivered dose, setup uncertainties and baseline variations have also to be taken into account when evaluating and accumulating the dose [10].

The aim of this study was to assess the effect of respiratory induced density variations by disentangling the effects of geometry and density variations on the dose

and consequently evaluating the necessity of a full 4D dose calculation in treatment-planning rather than only using geometry information. To do so, the static 3D planned dose was accumulated over the 4D trajectory. In this way only geometry variations were included while density variations were explicitly excluded, as depicted in Figure 7-1. Comparing the result with the full accumulated 4D dose singles out the effect of density variations on the dose distribution.

2. Methods and materials

2.1. Patient group

Ten patients who received radiotherapy for inoperable non-small-cell lung cancer were selected in this retrospective study, based on a clearly definable primary tumor exhibiting a large peak-to-peak respiration-induced motion (amplitudes ranged from 1.1 to 3.6 cm in cranio-caudal (CC) direction). In addition, a variety of tumor locations and sizes were chosen, while patients with nodal involvement were excluded (Table

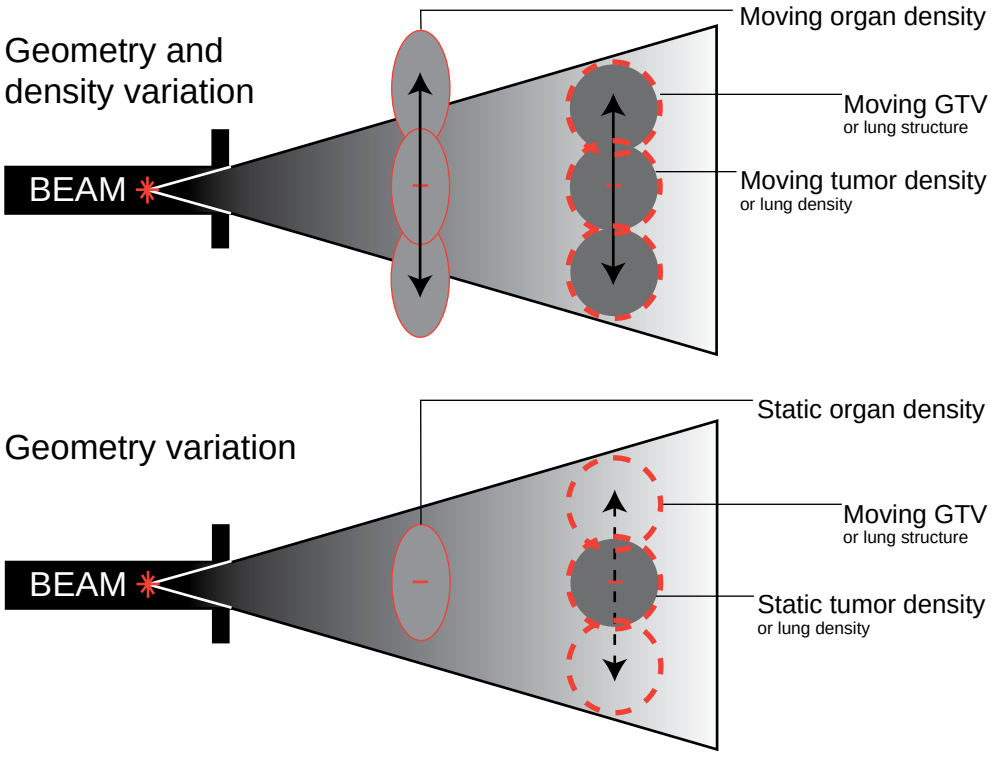

Figure 7-1. Schematic illustration of study setup to determine the influence of geometry and density variations on the delivered dose. (Top) Measuring the combined influence of geometry and density variations within the gross target volume (GTV) or lung structure. (Bottom) Measuring the influence of geometry variations within the GTV or lung structure. The difference between these two measurements represents the influence of the density variations.

7-1). The group, representing the top 30% of the motion generally observed in lung cancer patients [11], was selected to find an upper limit of the effect of respiratory motion. There are two treatment groups: Patients treated with conventional radiotherapy (CRT; patient 1-5) and stereotactic body radiotherapy (SBRT; patient 6-10). In each group, the patients are numbered according to increasing tumor motion.

2.2. Four-dimensional CT and mid-ventilation CT

For each patient a 4D CT scan in normal free breathing was acquired using a multislice CT scanner (24-slice Somatom Sensation Open, Siemens) in helical cardiac scanning mode.

Patient respiration was registered using a thermocouple inserted into the entry of a regular oxygen mask. The thermocouple respiratory signal was then used for data sorting. By dividing the respiratory cycle into ten equidistant time-percentage bins (0% at maximum-inhalation), ten time-sorted data sets, corresponding to the ten breathing phases, were reconstructed from the sinogram data.

Subsequently a single 3D mid-ventilation CT scan (MidV CT) was constructed for treatment-planning. For this purpose, first the tumor motion curve was obtained by rigid registration of a region encompassing the tumor in all ten CT frames to a reference CT frame [12]. From this motion curve the time-percentage in the exhalation part of the respiratory cycle was determined at which the tumor is closest to its time-weighted mean position. At this time-percentage (which does not need to be a multiple of 10%) the MidV CT was reconstructed from the 4D CT data [12].

Table 7-1 Tumor location (R=right-lung, L=left-lung, U=upper-lobe, L=lower-lobe), peak-to-peak tumor motion amplitude in CC (predominant motion direction), GTV (gross tumor volume) volume, treatment and clinically used margins for all ten patients.

Patient	Tumor location	Amplitude CC (cm)	Volume (cc)	Treatment	Clinically used margins (cm)		
					AP	CC	LR
1	LU	1.5	10	CRT	1.3	1.5	1.3
2	LU	1.9	60	CRT	1.3	1.7	1.2
3	LL	2.1	70	CRT	1.3	1.7	1.3
4	RL	2.4	10	CRT	1.3	1.8	1.3
5	RL	3.0	32	CRT	1.3	1.9	1.3
6	RU	1.1	6	SBRT	0.8	0.9	0.9
7	RU	1.4	9	SBRT	0.9	1.0	0.8
8	RU	1.7	14	SBRT	0.9	1.1	0.8
9	RL	2.0	30	SBRT	0.5	1.0	0.5
10	RL	3.6	13	SBRT	0.7	1.3	0.8

2.3. Treatment-planning

The MidV CT was used to delineate the GTV (no GTV-to-CTV margin) and OARs with in-house software, consecutively a treatment plan was created with the Pinnacle treatment-planning system (version 7.6, collapsed cone convolution superposition dose calculation algorithm). Patient-specific GTV-to-PTV margins were determined according to van Herk *et al.* (e.g., [205]) including setup and baseline uncertainties. These margins (Table 7-1) only moderately depend on the patient-specific peak-to-peak tumor amplitudes because the effect of this motion is the same as a random error (and low dose gradients in lung).

The conventional treatment plans for patients 1-5 (24 fractions of 2.75 Gy) consisted of six to seven coplanar beams. They were optimized such that 99% of the PTV received at least 90% of the prescribed dose of 66 Gy. The maximum PTV dose was required to be not more than 107% of the prescribed dose, while fulfilling usual dose limit constraints for the lung, spinal cord, oesophagus and heart. The GTV-to-PTV margins for this patient group ranged from 15 to 19 mm in the CC direction, which is the predominant motion direction.

In the SBRT plans for patients 6-10, also non-coplanar angles were utilized for the 16 to 18 beams. A dose of 54 Gy (3 fractions of 18 Gy) was prescribed to the iso-dose line encompassing 95% of the PTV. Additionally, 99% of the PTV was required to receive minimally 90% of the prescribed dose. In this case the dose distribution in the PTV was allowed to be less homogenous than in a conventional plan, with a maximum PTV dose of 165% of the prescribed dose. The GTV-to-PTV margin ranged from 9 to 13 mm in CC direction. Differences in margin between CRT and SBRT are mainly due to differences in the image-guided radiotherapy protocols and different dose constraints [13].

2.4. Deformable registration

A deformable registration method was applied, registering all ten frames of the 4D CT to a reference scan, thereby accounting for non-rigid changes in the lung due to breathing. The image registration was done using a phase-based optical flow motion estimation procedure [8,14] resulting in a 4D deformation vector field (4D DVF) which defines the motion of each voxel of all ten frames with respect to the reference frame/scan (Chapter 4). The MidV CT scan was chosen as the reference scan.

2.5. Accumulated dose over respiratory cycle

The treatment plans designed on the MidV CT were applied to all 10 frames of the 4D CT and the dose distributions were recalculated (the result is referred to as the 4D dose distribution).

To single out the effect of respiration-induced density variations, the accumulated dose over the respiratory cycle was calculated in two different ways. First, the 4D

dose distribution was warped to the MidV position by applying the 4D DVF described above, resulting in a deformed 4D dose, which was then accumulated over the respiratory cycle to yield the accumulated 4D dose. This result includes the influence of both geometry and density variation and is illustrated in the upper panel of Figure 7-2. The accumulation was performed by a time-weighted summation, with all ten phases equally weighted in time with a factor of 0.1 corresponding to the time-sorted nature of the data.

Second, the same procedure was repeated but now the 4D DVF was applied to the MidV dose, which was copied to each phase (i.e., the same dose for all breathing phases). The resulting deformed MidV dose was accumulated, giving the

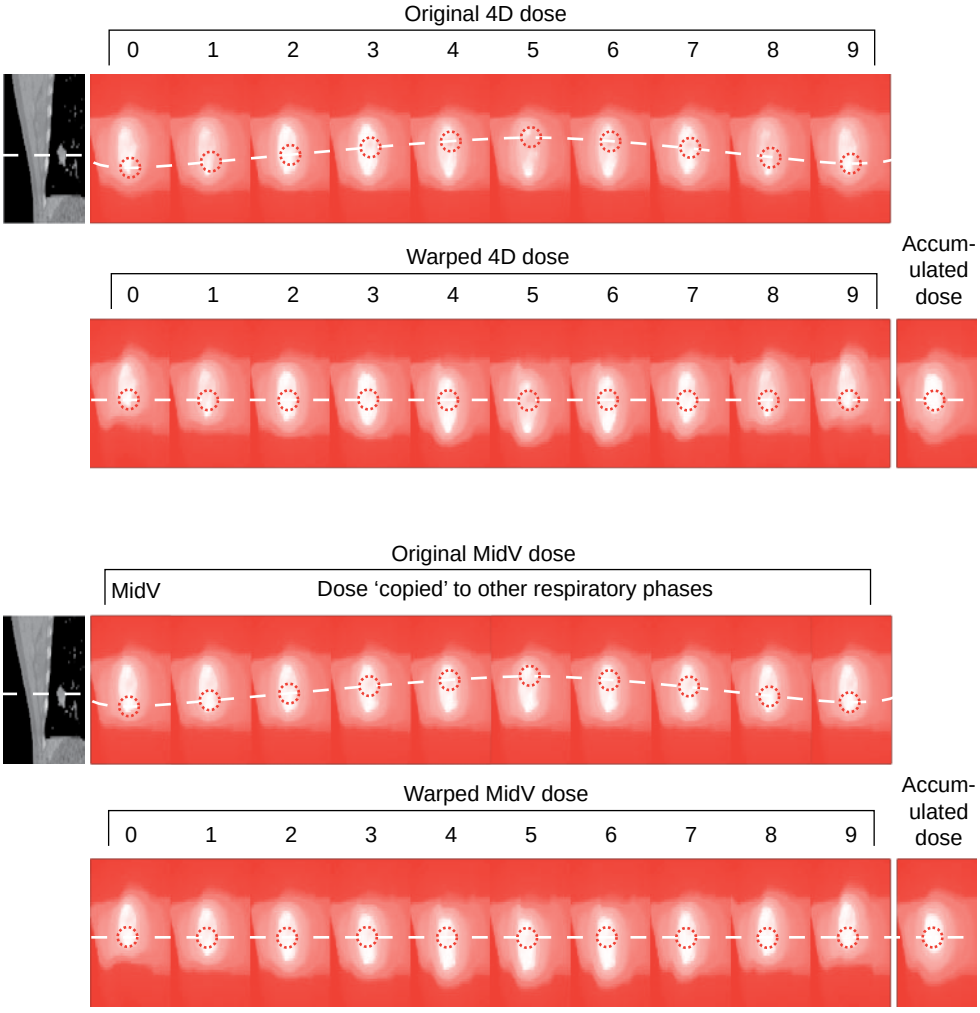

Figure 7-2. Example of a 4D, deformed 4D, and accumulated 4D dose (upper panel), and a MidV, deformed MidV, and accumulated MidV dose (lower panel). The white line indicates how the GTV moves within the dose, forming a 4D GTV trajectory over the respiratory cycle, while on the contrary the deformed dose moves around a static (MidV) GTV.

accumulated MidV dose (displayed in the lower panel of Figure 7-2). In this way, the geometry variations due to respiration are accounted for, while excluding any influence from the density variations.

In contrast, the planned dose as calculated on the MidV CT does not explicitly include information from neither density nor geometry variations (geometry variations in form of tumor motion are only indirectly taken into account in the PTV margin).

Figure 7-3 summarizes how the planned MidV dose –1–, the accumulated MidV dose –2–, and the accumulated 4D dose –3– are calculated. Note that the comparison between planned MidV dose –1– and accumulated 4D dose –3– does not explicitly tell you if the used GTV-to-PTV margin is adequate to cover the influence of respiration. To do so, not only the dose distributions corresponding to ten different respiratory phases have to be accumulated but also the dose distributions for differ-

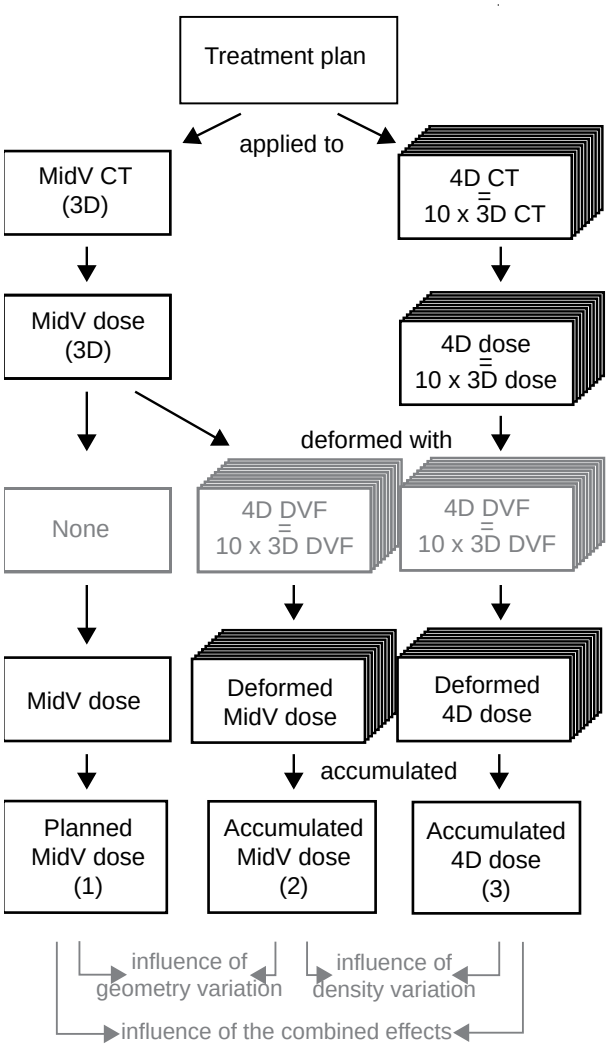

Figure 7-3. A schematic view of the methods to calculate (1) the (planned) MidV dose (left column), (2) the accumulated MidV dose (middle column), (3) the accumulated 4D dose (right column).

ent values of setup errors, baseline shifts, etc. Since this is not the aim of this study, only geometry and density variations due to respiratory motion were investigated.

2.6. Dose evaluation

To qualitatively investigate the effect of geometry and density variations on the dose, differences in dose per breathing phase and in cumulative dose were evaluated using isodose lines and DVHs. Furthermore, a quantitative analysis was performed for several clinically relevant treatment parameters: Generalized equivalent uniform dose (gEUD) of the GTV, mean lung dose (MLD), and the volume of the lung that gets at least 20 Gy (V20). To calculate the MLD and V20, a contour comprising the volume of both lungs minus the GTV volume was constructed (named Lungs).

3. Results

The patients were chosen such that they exhibited a variety of tumor amplitudes, locations and sizes (Table 1). However, since results (like isodoseline displays, DVHs, etc.) are comparable for all patients, they are only shown for one representative patient (patient 4 who exhibited a CC tumor motion of 2.4 cm –tumor was close to the diaphragm–). Summary results in terms of clinically relevant treatment parameters are given for all patients.

3.1. Dose distributions vs. breathing phase

Figure 7-4a–c shows isodose lines of the 4D dose in maximum-inhale and maximum-exhale and the MidV dose. The isodose lines hardly differ between breathing phases, and the most pronounced differences occur near the diaphragm. The deformed 4D and the deformed MidV dose (inhale and exhale for both cases) are shown in Figure 7-4d–g. The differences in dose distributions are noticeable between the different breathing phases of the deformed 4D dose (Figure 7-4d,e) or the deformed MidV dose (Figure 7-4f,g). However, the difference between the two deformed dose distributions are small (Figure 7-4d–g), which indicates that geometry variations over the respiratory cycle has a larger effect on the dose than density variations.

In Figure 7-5a,b the DVHs for the tumor (a) and the lungs (b) of the 10 phases of the deformed 4D dose are displayed. Some spread between the DVHs can be observed over the respiratory cycle. This spread ranges systematically for all patients from lower lung doses in inhale to higher lung doses in exhale. This systematic difference can be explained by the fact that in inhale the lung is maximally inflated therefore covering more lower dose regions, while in exhale the opposite effect takes place. No systematic pattern over the respiratory cycle can be found for the tumor DHVs.

In Figure 7-5c the DVHs for the tumor of the deformed MidV dose and of the deformed 4D dose are compared for maximum-inhale and maximum-exhale. The deformed 4D dose is slightly higher than the deformed MidV dose in these phases.

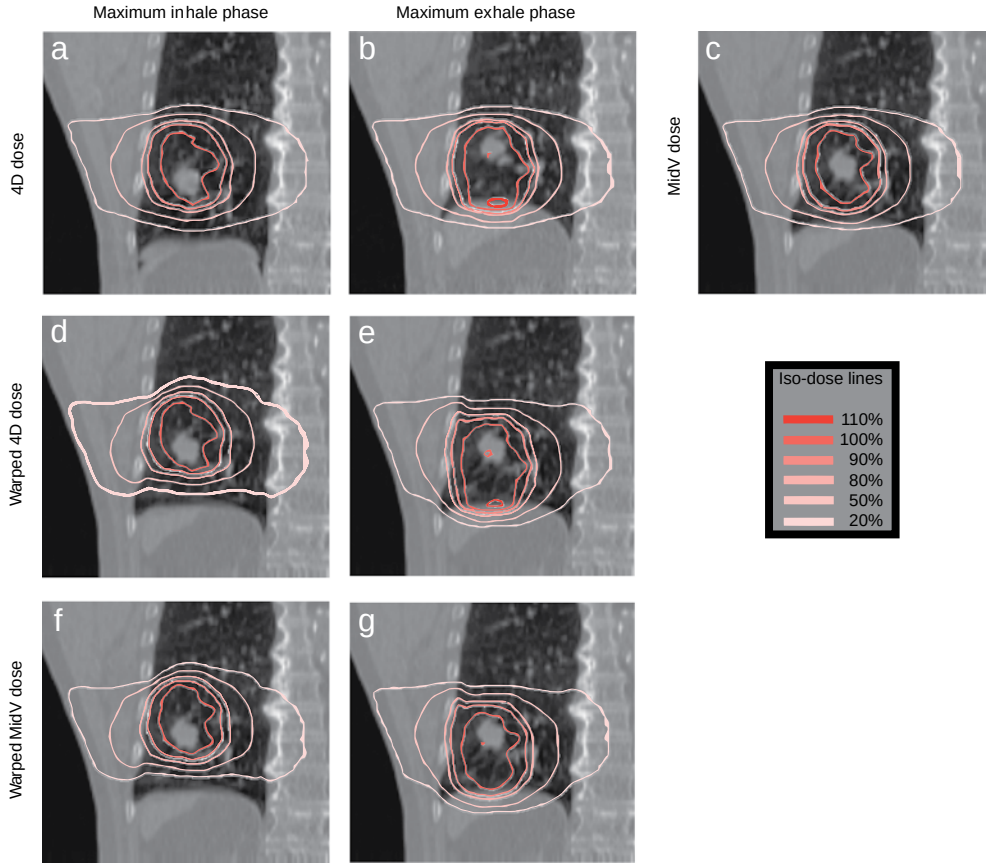

Figure 7-4. Isodose lines overlaid on CT for patient 4: (a,b) 4D dose – maximum-inhale phase/maximum-exhale phase, (c) MidV dose, (d,e) Deformed 4D dose – maximum-inhale phase/maximum-exhale phase, (f,g) Deformed MidV dose – maximum-inhale phase/maximum-exhale phase.

This was seen for all breathing phases, and all patients, demonstrating that the moving tumor density has a very small (but systematic) effect on the dose. In addition for the lung, the density variations have negligible impact on the overall lung dose (data not shown).

3.2. Accumulated dose over respiratory cycle

The tumor DVHs of the accumulated 4D dose and the accumulated MidV dose together with the planned MidV dose are shown in Figure 7-5d. These plots demonstrate that the small differences between deformed MidV dose and deformed 4D dose observed for the tumor in certain breathing phases become even smaller in the accumulated dose over the respiratory cycle. But still the accumulated 4D dose is slightly higher than the accumulated MidV dose. For the lung the two different cumulative doses are virtually identical (data not shown). This is also seen in Figure 7-5e,f where the mean tumor and the mean lung dose determined from the

deformed MidV and from the deformed 4D dose are plotted against the breathing phase. The mean doses determined from the accumulated MidV dose, the accumulated 4D dose and the planned MidV dose are also shown. These findings were very similar for all patients (Figure 7-6). On average over all patients, the difference in mean GTV dose between planning, accumulated MidV and accumulated 4D is less than 1%. For the lung dose, this difference is even less than 0.5%.

Figure 7-7a shows the relative difference in the gEUD of the tumor between the accumulated MidV and the accumulated 4D dose for all ten patients, $\Delta gEUD=(gEUD_{MidV}-gEUD_{4D})/gEUD_{4D}$. The gEUD is calculated with $a=-\infty$ (equivalent to minimum dose) and a=1 (equivalent to mean dose) as extremes in the possible gEUD values. For a=−10 often used for tumors, the gEUD is close to the minimum dose. The observed differences are mostly below 1%, both for the conventionally treated group (patients 1-5) and for the group with stereotactic treatment (patients 6-10). Even the largest relative difference for minimum tumor dose which is calculated for patient 10 who exhibited a tumor motion of 3.6cm CC is not more than 2%. Results of the gEUD of the tumor between planned and accumulated 4D dose are not extensively given (see Section 7-4.5) since the differences depend on the margin used, while setup uncertainties and baseline shifts were not considered in the accumulation.

An equivalent plot of the MLD and the V20, Figure 7-7b, shows even smaller relative differences for all patients, which are well below 0.5% for MLD, and not more than about 1% for V20.

4. Discussion

This study shows that the effect of respiration-induced density variations on the GTV dose accumulated over the respiratory cycle is very small for all patients analyzed, even in the presence of extreme lung tumor motion. This is concluded from the fact that accumulating on the planned MidV dose results in dose distributions very close to those accumulated on the 4D dose (Figure 7-4, Figure 7-5d). For clinically relevant treatment parameters, such as minimum tumor and mean lung dose, this effect can be neglected (Figure 7-7). For other OARs not described in this study, i.e., heart or oesophagus, comparable small effects as for lung are expected since they exhibit smaller respiration-induced motion and deformation and lie in regions of more homogeneous density. Since the influence of the density variations on the (4D) dose distributions is very small, it is expected that incorporating the density variations into the optimization of the treatment plan has very limited impact and is therefore not very useful.

The accuracy of the results in this study depends on the dose calculation algorithm and the deformable registration method. The collapsed cone dose calculation algorithms used in this analysis has proven in multiple studies to be better suited

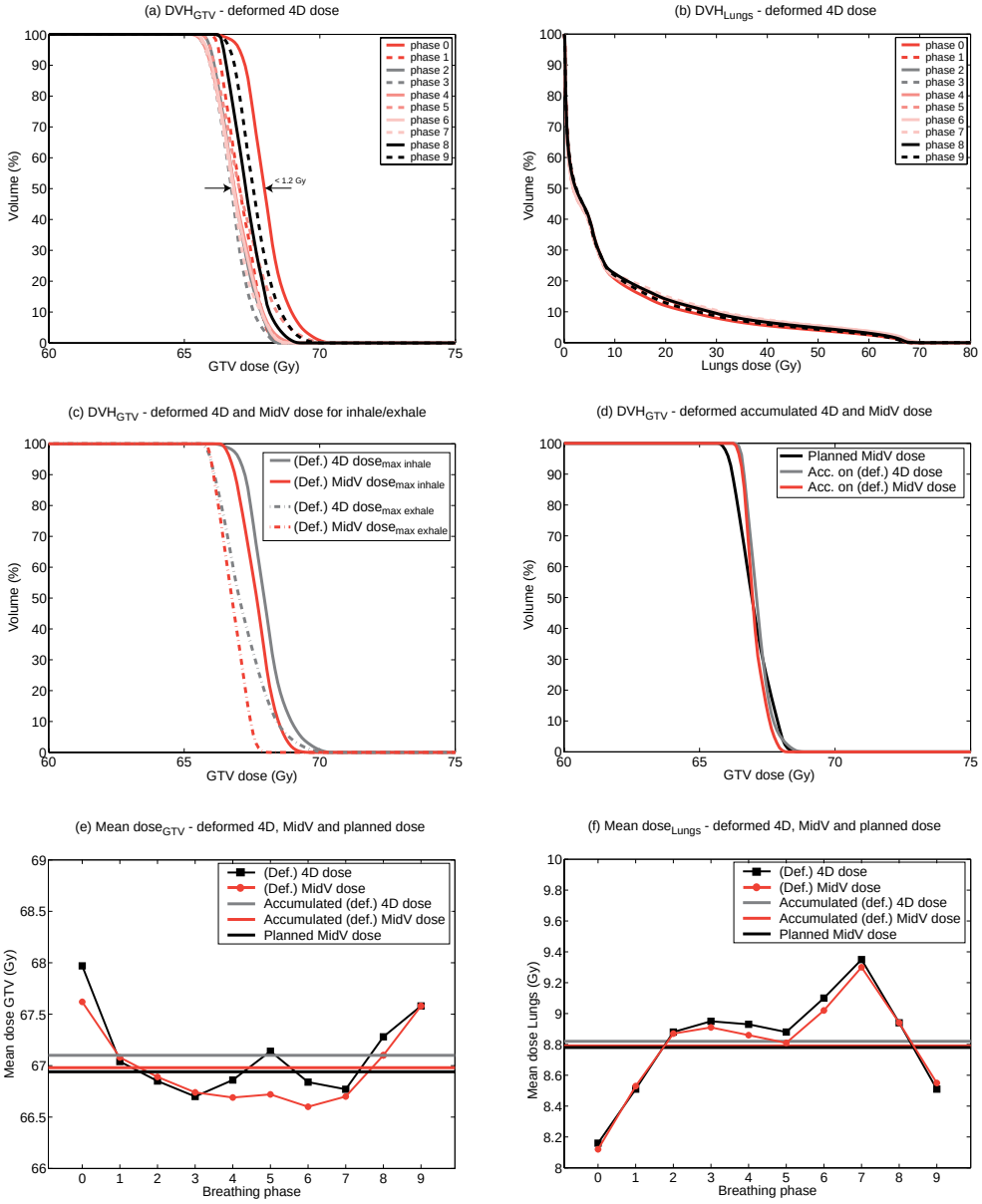

Figure 7-5. All plots from patient 4 (2.4cm cranio-caudal tumor motion). (a) DVH of the deformed 4D dose in all phases within the GTV. (b) DVH of the deformed 4D dose in all phases of the lung volume minus GTV. The deformed 4D and MidV dose in exhale and inhale (c) and accumulated over the respiratory phases (d). (e) The mean dose to the GTV from the deformed 4D and MidV dose as well as the planned dose over the respiratory cycle. (f) Same as (e) but for lung volume minus GTV.

for inhomogeneous tissues than the pencil beam algorithm, and nearly as good as Monte Carlo calculations (e.g., [15]). The accuracy of the deformable image registration was determined to be of the order of 1 mm (1SD) in all directions [8], thus demonstrating an excellent performance. The results of this study can therefore be considered to not be influenced by an insufficient dose calculation algorithm or registration procedure.

4.1. Dose tracks tumor

The accumulated 4D dose for the tumor was slightly higher than the accumulated MidV dose. This higher dose can be explained by the higher density in tumor than in lung tissue. The accumulated 4D dose (representing the actually received dose in the presence of just breathing and no other uncertainties) was determined within the tumor contour enclosing tumor tissue (Figure 7-1, upper part) in contrast to the tumor contour enclosing (partly) lung tissue in the accumulated MidV dose (Figure 7-1, lower part), resulting in a higher absorbed dose. In other words, the dose, to a some degree, *"tracks"* the tumor (this is also seen in e.g., [9]).

4.2. Conventional RT vs. SBRT

The small influence of density variations applies to both conventionally treated and SBRT patients. The differences in tumor dose between the accumulated MidV and accumulated 4D dose were slightly more pronounced for the SBRT group (patients 6-10 in Figure 7-7). This can be associated with the more inhomogeneous PTV doses and the smaller GTV-PTV margins in this group which in the region of steeper dose gradients make it more predisposed to a possible effect of density changes on the dose. The effect of density variations on the lung dose was negligible in both groups.

4.3. Patient selection

The patients were selected by reason of large tumor motion since these are the cases for which one expects the largest possible effect of respiration-induced density variations. However, the vast majority of the patients (about 70% [11]) exhibits tumor motions smaller than those in this study. Therefore the very small and in general negligible effect seen in this study can be considered an absolute upper limit for the entirety of all lung cancer patients.

4.4. Recalculation of the data using simplified methods

To investigate how the results behave if the analysis is further simplified, the determination of the cumulative tumor doses was repeated with a local rigid registration [16] of the region encompassing the tumor, justified by the observation that lung tumors in general are rather rigid compared to the surrounding lung. The tumor in each CT

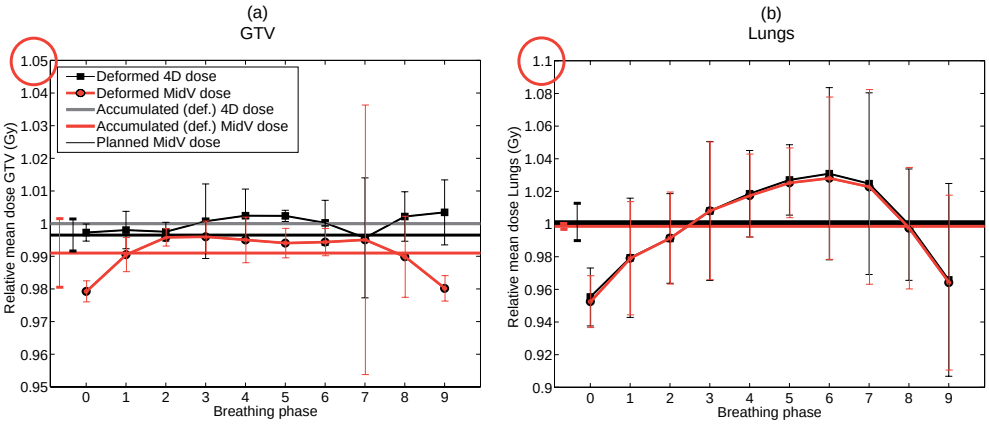

Figure 7-6. Relative mean doses for (a) GTV and (b) Lung (minus GTV) averaged over all patients. The values are relative the accumulated 4D dose (which is considered as "truth"). The error bars represent the standard deviation over the 10 patients in this study. The relatively large error bar at phase 7 is due to a single (relative) large deviation from the mean of one patient.

of the 10 breathing phases was matched to its position in the MidV CT, allowing only translations. The cumulative tumor dose was calculated by shifting the MidV and the 4D dose respectively for each phase according to this tumor trajectory, and accumulating over all phases. The resulting cumulative dose distributions were nearly identical to those obtained when using deformable registration (differences<0.5%). As an alternative to the MLD of the accumulated dose obtained with deformable registration, the lungs were automatically segmented on all breathing phases, the MLDs within these contours were determined, and then the mean of the MLDs over all breathing phases was calculated, neither giving any significant deviations (<0.5%).

4.5. Comparison with other literature

The studies of Guckenberger *et al.* [17] and Rosu *et al.* [18] compare the 4D dose accumulated over the respiratory cycle to the planned dose. This is, however, not a completely correct comparison because the used PTV accounts for other geometrical uncertainties as well. The comparison will show the influence of the combined effect of respiration-induced geometry and density variations but it does not tell explicitly if the used GTV-to-PTV margin is adequate to cover setup errors and baseline shifts in the presence of breathing motion. On the contrary, focusing on the influence of breathing motion by setting the GTV/ITV-to-PTV margin to zero (i.e., ignoring other uncertainties) [9], will overestimate the influence of breathing [13] since error contributions (as being a probability) are summed quadratically [20]. In addition, dose planning without an uncertainty margin is clinically irrelevant.

The above-mentioned studies used a considerably large PTV (including ITV approach covering the complete tumor motion and thereby overestimating the effect of breathing [19]). As a result the tumor (or GTV) moves within a homoge-

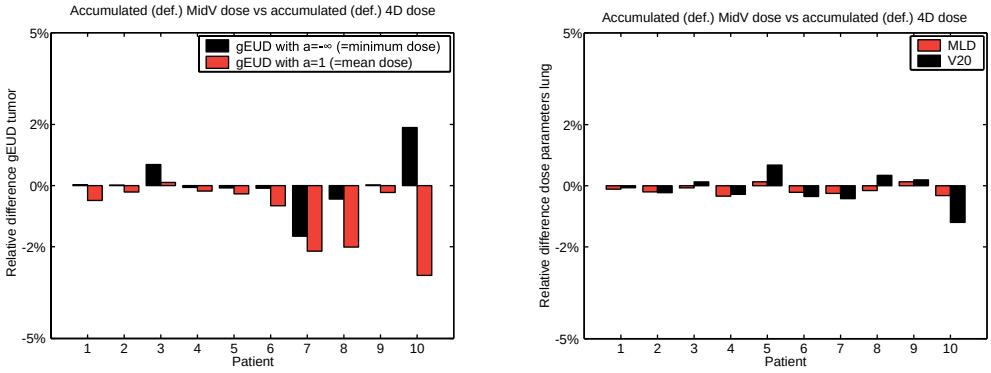

Figure 7-7. Relative difference in tumor gEUD (a) and MLD and V20 (b) between accumulated MidV dose and accumulated 4D dose for all patients. Patients 1-5 treated conventionally, patients 6-10 stereotatically, in each group numbering according to increasing tumor motion.

neous dose region and therefore only small differences between planned and accumulated GTV dose due to the geometry [20] and density variations (this chapter) is expected. Using smaller PTVs (as described in Section 7-2.3 and Chapter 3 [12]) the impact of geometry variation increases (see below) while the impact of density variations remains limited. Still performing the comparison of planned MidV to the accumulated 4D dose for the present study results in relative differences of the planned dose versus the accumulated 4D dose between -0.1% and -1.7% for the mean GTV dose, and between +0.6% and -7.9% % for the minimum GTV dose for patients 1-9. For patient 10 with a very large tumor motion (3.6 cm peak-to-peak) the highest difference in minimum GTV dose of +19.5% is seen while the difference in mean GTV dose is only +0.1%. This large dose difference was anticipated as in this case respiratory motion by far exceeded other uncertainties (i.e., planned minimum dose to the PTV equals minimum accumulated dose to the GTV).

Guckenberger *et al.* [17] reported larger differences in GTV dose between 4D and static dose in the exhale phase (similar findings were reported by Rosu *et al.* [18]). However, in that study, the dose comparison was done between calculations with tumor tissue in the exhale position and in the inhale position respectively. This represents larger density differences than in our study, which compares tumor tissue in exhale vs. in MidV position. Planning on the MidV CT ensures an appropriate representation of the mean geometry and density of the patient, especially an accurate estimate of the mean position and shape of the tumor and the lungs. When planning on the exhale CT this is not the case. For example, it was seen (Figure 7-5b,f) that the lung dose is nearly always largest in exhale, which introduces a (generally overestimating) bias in the estimate of the lung dose using an exhale CT.

5. Conclusions

This study has shown that although density variations due to respiration-induced tumor motion lead to some variations in the dose distribution over the respiratory cycle, the influence on the accumulated dose is very small. A full 4D dose calculation in treatment-planning does therefore not seem to be required. Planning on a MidV CT derived from a 4D CT and taking motion and deformation into account by deforming the MidV dose (or even using rigid registration) is a very good estimate of the overall effect of respiration on the cumulative dose received by the tumor and the lungs.

As a result, using a single (static) MidV CT scan with an appropriate margin (including margins for setup errors, baseline variations and breathing), the influence of geometry and density variations is small and therefore, it implies that this MidV approach is safe to use.

References

1. Rosu M, Chetty I J, Balter J M et al., “Dose reconstruction in deforming lung anatomy: dose grid size effects and clinical implications”, Med.Phys. 2005;32:2487-2495
2. Keall PJ, Cattell H, Pokhrel D et al., “Geometric accuracy of a real-time target tracking system with dynamic multileaf collimator tracking system”, Int.J.Radiat.Oncol.Biol.Phys. 2006;65:1579-1584
3. Nioutsikou E, Seppenwoolde Y, Symonds-Tayler J R et al., “Dosimetric investigation of lung tumor motion compensation with a robotic respiratory tracking system: an experimental study”, Med.Phys. 2008;35:1232-1240
4. Tewatia D, Zhang T, Tome W et al., “Clinical implementation of target tracking by breathing synchronized delivery”, Med.Phys. 2006;33:4330-4336
5. Vedam SS, Keall P J, Kini V R et al., “Acquiring a four-dimensional computed tomography dataset using an external respiratory signal”, Phys.Med.Biol. 2003;48:45-62
6. Nijkamp J, Wolthaus J W H, Sonke J J et al., “Mid-ventilation Determination with Automatic Four-dimensional Rigid Grey-value Registration on Respiration-correlated Computed Tomography Scans with Moving Lung Tumours”, Proceedings of the XVth ICCR - Toronto - Canada 2007;
7. Brock KK, Dawson L A, Sharpe M B et al., “Feasibility of a novel deformable image registration technique to facilitate classification, targeting, and monitoring of tumor and normal tissue”, Int.J.Radiat.Oncol.Biol.Phys. 2006;64:1245-1254
8. Wolthaus JWH, Sonke J J, Herk M v et al., “Motion Estimation and Compensating in 4D CT Images using Phase-based Constraint Models “, Proceedings of the XVth ICCR - Toronto - Canada 2007;
9. Admiraal MA, Schuring D, and Hurkmans C W, “Dose calculations accounting for breathing motion in stereotactic lung radiotherapy based on 4D-CT and the internal target volume”, Radiother. Oncol. 2008;86:55-60
10. Engelsman M, Damen E M, De Jaeger K et al., “The effect of breathing and set-up errors on the cumulative dose to a lung tumor”, Radiother.Oncol. 2001;60:95-105
11. Sonke JJ, Lebesque J, and van Herk M., “Variability of four-dimensional computed tomography patient models”, Int.J.Radiat.Oncol.Biol.Phys. 2008;70:590-598
12. Wolthaus JW, Schneider C, Sonke J J et al., “Mid-ventilation CT scan construction from four-dimensional respiration-correlated CT scans for radiotherapy planning of lung cancer patients”, Int.J.Radiat.Oncol.Biol.Phys. 2006;65:1560-1571
13. van Herk M, “Teaching Session: 4D Radiotherapy”, Clin.Oncol.(R.Coll.Radiol.) 2007;19:S16-
14. Hemmendorff M, Andersson M T, Kronander T et al., “Phase-based multidimensional volume registration”, IEEE Trans.Med.Imaging 2002;21:1536-1543
15. Vanderstraeten B, Reynaert N, Paelinck L et al., “Accuracy of patient dose calculation for lung IMRT: A comparison of Monte Carlo, convolution/superposition, and pencil beam computations”, Med.Phys. 2006;33:3149-3158
16. Roche A, Pennec X, Malandain G et al., “Multimodal Image Registration by Maximization of the Correlation Ratio”, Rapport de Recherche, Institut National de Recherche Informatique et en Automatique 1998;3378:
17. Guckenberger M, Wilbert J, Meyer J et al., “Is a single respiratory correlated 4D-CT study sufficient for evaluation of breathing motion?”, Int.J.Radiat.Oncol.Biol.Phys. 2007;67:1352-1359
18. Rosu M, Balter J M, Chetty I J et al., “How extensive of a 4D dataset is needed to estimate cumulative dose distribution plan evaluation metrics in conformal lung therapy?”, Med.Phys. 2007;34:233-245
19. Wolthaus JWH, Sonke J J, Herk M v et al., “Comparison of different strategies to use four-dimensional computed tomography in treatment planning for lung cancer patients”, Int.J.Radiat.Oncol.Biol.Phys. 2008;70:1229-1238
20. van Herk M, Remeijer P, Lebesque JV., “Inclusion of geometric uncertainties in treatment plan evaluation.” Int.J.Radiat.Oncol.Biol.Phys. 2002;52:1407-1422.